

## **General Disclaimer**

### **One or more of the Following Statements may affect this Document**

- This document has been reproduced from the best copy furnished by the organizational source. It is being released in the interest of making available as much information as possible.
- This document may contain data, which exceeds the sheet parameters. It was furnished in this condition by the organizational source and is the best copy available.
- This document may contain tone-on-tone or color graphs, charts and/or pictures, which have been reproduced in black and white.
- This document is paginated as submitted by the original source.
- Portions of this document are not fully legible due to the historical nature of some of the material. However, it is the best reproduction available from the original submission.

NASA Technical Memorandum 82947

(NASA-TM-82947) ADVANCES IN CORE LOSS  
CALCULATIONS FOR MAGNETIC MATERIALS (NASA)  
33 p HC A03/MF A01

CSCL 09C

N83-11446

Unclassified  
G3/33 0 1007

# Advances in Core Loss Calculations for Magnetic Materials



James E. Triner  
*Lewis Research Center*  
*Cleveland, Ohio*

Prepared for the  
Fall Meeting of the American Ceramic Society  
Cambridge, Massachusetts, September 12-15, 1982

NASA

## Advances in Core Loss Calculations for Magnetic Materials

James E. Triner

National Aeronautics and Space Administration  
Lewis Research Center  
Cleveland, Ohio 44135

### Abstract

This paper describes a new analytical technique which predicts the basic magnetic properties under various operating conditions encountered in state-of-the-art dc-ac/dc converters. Using a new flux-controlled core excitation circuit, magnetic core characteristics were developed for constant values of ramp flux (square wave voltage excitation) and frequency. From this empirical data, a mathematical loss characteristics equation is developed to analytically predict the specific core loss of several magnetic materials under various waveform excitation conditions. In addition, these characteristics show the circuit designer for the first time the direct functional relationships between induction level and specific core loss as a function of the two key dc-dc converter operating parameters of input voltage and duty cycle.

### I. Introduction

Magnetic materials offer the power electronics designer a wide range of magnetic characteristics from which he must select those materials applicable to his particular dc-ac/dc converter design. Like their semiconductor counterparts, magnetic devices display families of operating characteristics which are functions of frequency, temperature, basic material composition, fabrication techniques, and driving source impedance<sup>1</sup>. The interaction between these various functions may be explained by ferromagnetism, material properties, or domain wall movement<sup>2</sup>. However, for power electronics applications it is desirable to provide a set of magnetic characteristics which are easily

understood and accurately predict the performance of a particular magnetic material when applied in a specific dc-ac/dc converter configuration. This paper examines the loss characteristics of several magnetic materials used in present state-of-the-art power processing circuits. The effects of variables such as frequency, voltage level, voltage waveforms and modulation upon the inherent material characteristics are explored using only externally measurable quantities.

Traditionally derived sinusoidal core-loss characteristics for a particular magnetic material and lamination thickness are generally available (as shown in Fig. 1) with flux density as the independent variable, specific core loss (SCL) as the dependent variable, and frequency as a parameter<sup>3</sup>. Only recently has attention been given to the different loss characteristics (Figs. 2(a) and (b)) of magnetic materials observed between sinusoidal and square wave excitation conditions at 10 000 Hz.

Some insight as to this loss difference may be explained by examining the superimposed B-H characteristics (Fig. 2 (c)), and the instantaneous flux displayed as a function of time. The following qualitative observations may be made: Since  $B_M$  is held constant, hysteresis loss is constant, and eddy current loss is dependent only upon  $d\phi/dt$ . At point 1,  $d\phi/dt$  of the sine wave is equal to zero while  $d\phi/dt$  of the square wave is equal to some positive constant value. Therefore, the core loss for the square wave at point 1 is greater (wider B-H loop width) than that for the sine wave at point 1. As the flux density increases to point 2,  $d\phi/dt$  for the sine wave reaches its maximum value. This value of  $d\phi/dt$  is greater than the  $d\phi/dt$  for the square wave, and the corresponding core loss (B-H width) is greater. As the flux density increases to point 3,  $d\phi/dt$ 's for the sine and square wave are

approximately equal as shown by the equal B-H widths. Again as the flux approaches point 4, the same conditions as point 1 are repeated.

The square wave B-H loop and associated core-loss characteristics may be observed in a unique manner by using a test circuit in which the flux rate of change ( $d\phi/dt$ ) is observed as the independent variable, and the power loss is measured using a wide bandwidth (dc-300 kHz) wattmeter. This excitation circuit allows the control of an additional variable,  $d\phi/dt$ , rather than just the driving frequency, as is the case for all previous sinusoidal core-loss measurements. Data collected with the new excitation circuit are based upon values of constant  $d\phi/dt$  which corresponds with square wave excitation. The core-loss characteristics are shown in Fig. 3 with frequency as the independent variable, SCL as the dependent variable, and  $d\phi/dt$  and flux density as parameters.

In all the SCL characteristics presented, both positive and negative values of  $d\phi/dt$  were held constant over one cycle. These  $d\phi/dt$  conditions allow symmetrical square wave voltage excitation of the magnetic material under test. With the data recorded in this manner, Faraday's Law ( $e = -Nd\phi/dt$ )<sup>5</sup> is then used to calculate the  $d\phi/dt$  value directly using the excitation voltage level, and the number of turns on the core. Using square wave excitation allows a direct separation of variables because  $d\phi/dt$  is a constant value. However, for sinusoidal excitation,  $d\phi/dt$  is a constantly changing over the cycle. In an actual dc-dc converter application the excitation voltage level is the input voltage being applied to a particular magnetic device.

Analytical prediction of core loss in magnetic materials is important from both an economic<sup>6</sup> and an engineering design<sup>7</sup> standpoint. Accurate

prediction allows design tradeoffs to be made between the areas of weight, efficiency, and performance. In addition, new circuit developments employing magnetic devices may be more fully analyzed without costly hardware fabrication. Early work<sup>8</sup> at frequencies of up to 200 kHz was aimed at measuring the magnetic properties of iron. Separation of core loss into its specific components of eddy current, static hysteresis, and anomalous loss has been examined more recently in great depth<sup>9 to 11</sup> for low frequency (<1 kHz) sinusoidal excitations.

With the growth of power electronics to higher power levels, and the employment of new converter techniques, the need to understand the properties of magnetic materials under high-frequency nonsinusoidal conditions is arising.

## II. Analytical Calculation Methods

Using the SCL characteristics for square wave excitation, three methods were developed which analytically predict the SCL of a magnetic material for pulse-width modulated square wave excitation. These methods are discussed in detail below.

### (1) Specific Core Loss Based on $B_M$ of the Core

The SCL characteristics presented in Fig. 3 relate the total specific loss (hysteresis + eddy current = total loss) to frequency with  $B_M$  as a parameter. This data will be used to determine the core-loss characteristics with pulse-width modulated square wave core excitation. This method is the most indirect approach to calculating the SCL. It requires an accurate measure of the effective cross-sectional area of the core. Generally, however, this is a parameter which is not accurately known to the power electronics designer.

Figure 4 shows the oscilloscope traces of a 1000 Hz square wave operating over a duty-cycle range of 10 to 50 percent. For each duty cycle the voltage for the positive cycle is adjusted to a maximum value of 4 V. The DC offset

in the core is held to a minimum. Therefore, the negative and positive half cycle V-sec are equal.

In order to use the Fig. 3 characteristics the  $B_M$  value for each duty-cycle condition must be determined. This value may be obtained as follows:

From Faraday's law

$$e_c = -Nd\phi/dt \text{ (V)} \quad (1)$$

Therefore

$$d\phi/dt = -e_c N^{-1} \text{ (We/sec)} \quad (2)$$

For each cycle portion

$$\Delta\phi = (d\phi/dt) \Delta t \quad (3)$$

$$\Delta\phi = -e_c N^{-1} \Delta t \quad (4)$$

and,

$$B_M = \Delta\phi (2A_e)^{-1} = -0.5e_c \Delta t (NA_e)^{-1} \text{ (T)} \quad (5)$$

where:

$$A_e = A_c \times SF \text{ (M}^2\text{)}$$

N = number of turns

$e_c$ ,  $\Delta t$  + related to duty cycle

Using 12.7  $\mu\text{m}$  (1/2 mil) Supermalloy as an example, for a frequency of 1000 Hz, the  $B_M$  values corresponding to each duty cycle width can be determined as follows:

$$B_M \text{ (positive cycle)} = -0.5(3.9)(100 \times 10^{-6})(10 \times 1.97 \times 10^{-4})^{-1} \\ = 0.099 \text{ T}$$

$$B_M \text{ (negative cycle)} = -0.5(-0.44)(900 \times 10^{-6})(10 \times 1.97 \times 10^{-4})^{-1} \\ = 0.1 \text{ T}$$

$$B_M \text{ (positive cycle)} \approx B_M \text{ (negative cycle)}$$

Considering the positive half cycle only this calculation can be repeated for the remaining four cases with the results shown below:

| Duty cycle,<br>percent | $\Delta t - \mu s$ | $e_c^+ / V$ | $B_m^+ / T$ |
|------------------------|--------------------|-------------|-------------|
| 10                     | 100                | 3.9         | 0.099       |
| 20                     | 200                | 3.9         | 0.198       |
| 30                     | 300                | 3.9         | 0.297       |
| 40                     | 400                | 3.9         | 0.386       |
| 50                     | 500                | 3.9         | 0.432       |

ORIGINAL PAGE IS  
OF POOR QUALITY

This data can now be used with Fig. 3 to determine the SCL associated with each duty-cycle condition. The results of these calculations are shown in Fig. 5.

During the experiment the SCL was measured for each duty-cycle condition. A comparison between the measured and calculated results is shown in Fig. 6. At the 50 percent duty-cycle condition the error between the measured and calculated SCL was:

$$SCL_{calc} = 0.682 W/kg$$

$$SCL_{meas} = 0.746 W/kg$$

$$\text{percent error} = \frac{SCL_{meas} - SCL_{calc}}{SCL_{meas}} \times 100 \quad (6)$$

$$\text{percent error} = \frac{0.746 - 0.682}{0.746} \times 100 = 8.6 \text{ percent}$$

From these results it may be seen that the SCL can be easily calculated for pulse-width modulated square waves if the base frequency, excitation voltage level, duty-cycle, number of turns, and the effective cross-section area of the core are known. Also, for a constant input voltage as the duty cycle increases,  $B_m$  increases, and the SCL of the magnetic device increases.

## (2) Specific Core Loss Based on $d\phi/dt$ in the Core

The SCL characteristics presented in Fig. 3 relate the total SCL to frequency with  $B_M$  and  $d\phi/dt$  as parameters. If the  $B_M$  parameter is ignored on this figure, the SCL can be calculated by using the  $d\phi/dt$  parameter and an equivalent excitation frequency. For a pulse-width modulated square wave with a constant positive  $d\phi/dt$  and a constant negative  $d\phi/dt$ ,  $B_M$  is determined directly by the length of time that the pulse is on. The width of this "on pulse" has an "equivalent" frequency of

$$f_{eq} = T_{eq}^{-1} = (2t_{on})^{-1} \quad (7)$$

Also, it was shown that the total SCL per cycle could be broken down into a half cycle loss dependent on  $d\phi/dt$ . Therefore, the total SCL may be determined using the following relationship.

$$\text{Total SCL} = (\text{SCL}/\text{cycle}) (\text{excitation frequency}) \equiv \text{SCL}_T$$

$$\text{SCL}_T = \left( \frac{1}{2} \frac{\text{SCL}^+}{f_{eq}^+} + \frac{1}{2} \frac{\text{SCL}^-}{f_{eq}^-} \right) f_{ex} \quad (8)$$

where

$\text{SCL}^+$  positive cycle SCL

$\text{SCL}^-$  negative cycle SCL

$f_{eq}^+$  positive cycle equivalent frequency

$f_{eq}^-$  negative cycle equivalent frequency

$f_{ex}$  excitation frequency

Example:

10 percent duty-cycle case:

$$e_c^+ = 3.9V$$

ORIGINAL PAGE IS  
OF POOR QUALITY

ORIGINAL PAGE IS  
OF POOR QUALITY

$$e_c^- = 0.44V$$

$$f_{ex} = 1000 \text{ Hz}$$

$$t_{on}^+ = 100 \times 10^{-6} \text{ sec}$$

$$t_{on}^- = 900 \times 10^{-6} \text{ sec}$$

Then

$$f_{eq}^+ = (2t_{on}^+)^{-1} = (2 \times 100 \times 10^{-6})^{-1} = 5 \text{ kHz}$$

$$f_{eq}^- = (2t_{on}^-)^{-1} = (2 \times 900 \times 10^{-6})^{-1} = 555 \text{ Hz}$$

using Faraday's law

$$d\phi/dt = e_c N^{-1}$$

$$(d\phi/dt)^+ = 3.9(10)^{-1} = 0.390 \text{ We/sec}$$

$$(d\phi/dt)^- = 0.44(10)^{-1} = 0.044 \text{ We/sec}$$

Replotting Fig. 3 as Fig. 7 with  $(d\phi/dt)^+$ ,  $(d\phi/dt)^-$ ,  $f_{eq}^+$ , and  $f_{eq}^-$  shown, the corresponding SCL's may be read directly from the figure:

$$\text{SCL}^+ = 0.180 \text{ W/kg}$$

$$\text{SCL}^- = 0.014 \text{ W/kg}$$

Using the equation for the total SCL the following results are obtained:

$$\text{SCL}_T = \frac{1}{2} \left( \frac{0.180}{5000} + \frac{0.014}{555} \right) 1000$$

$$\text{Total SCL} = 0.031 \text{ W/kg}$$

summarizing the results for the other conditions we have:

$f_{\text{base}} = 1000 \text{ Hz}$ 

| Duty cycle,<br>percent | $f_{\text{eq}}^+$ ,<br>Hz | $f_{\text{eq}}^-$ ,<br>Hz | $\frac{d\phi}{dt}^+$<br>We/sec | $\frac{d\phi}{dt}^-$<br>We/sec | $SCL^+$ ,<br>W/kg | $SCL^-$ ,<br>W/kg | $SCL_T$<br>W/kg |
|------------------------|---------------------------|---------------------------|--------------------------------|--------------------------------|-------------------|-------------------|-----------------|
| 10                     | 5000                      | 555                       | 0.39                           | 0.044                          | 0.181             | 0.014             | 0.031           |
| 20                     | 2500                      | 625                       | 0.39                           | 0.10                           | 0.356             | 0.061             | 0.119           |
| 30                     | 1670                      | 714                       | 0.39                           | 0.16                           | 0.528             | 0.163             | 0.273           |
| 40                     | 1250                      | 833                       | 0.38                           | 0.26                           | 0.660             | 0.422             | 0.517           |
| 50                     | 1000                      | 1000                      | 0.34                           | 0.34                           | 0.660             | 0.660             | 0.660           |

In Fig. 8 these calculated SCL's are compared with the measured SCL values for these duty-cycle conditions. The percent error is the same as obtained with method 1 (8.6 percent).

### (3) Specific Core Loss Based on Incremental $d\phi/dt$ in the Core

The technique developed in method 2 allows determination of the SCL based on the  $d\phi/dt$  value for the entire positive or the entire negative cycle of the square wave.

For a particular frequency and  $B_M$  level a family of curves could be developed for various  $d\phi/dt$  values as shown in Fig. 9. Using actual square waves observed in this experiment (Fig. 4), it can be seen that for any interval the actual exciting voltage is not a constant value. This would indicate that the corresponding  $d\phi/dt$  values over the cycle are not of constant value. If the waveform is broken down into discrete sample intervals, the corresponding locus of points on the B-H loop may be plotted as  $\Delta t$  is incremented. The corresponding B-H width would be a direct function of the pulse height for that interval. Figure 9(b) shows how the pulse height,  $d\phi/dt$ , and  $\Delta t$  would translate into a locus of points on the B-H loop. This approach may be used to explain the B-H loop shapes observed under various excitation conditions.

Relating these various  $d\phi/dt$  rates to loss at the positive equivalent frequency, the SCL characteristics of Fig. 9(c) may be used to determine the incremental core loss.

The loss per interval is calculated as follows:

$$T^+ = n \Delta t_i^+ = \frac{1}{2f^+} \quad (9)$$

where  $n$  = number of increments

$$\Delta t_i^+ = \frac{1}{2nf^+} \quad (10)$$

The energy dissipated in  $\Delta t_i^+$  would be:

$$\Delta E_i^+ = SCL_i^+ \Delta t_i^+ = \frac{SCL_i^+}{2nf^+} \quad (11)$$

If  $\Delta t_i^+$  were made small enough, the difference between the incremental excitation would approach zero as a limit.

The total energy over the positive cycle is simply the summation of the incremental  $\Delta E^+$ 's:

$$E_T^+ = \sum_{i=1}^N \Delta E_i^+ = \frac{1}{2nf^+} \sum_{i=1}^n SCL_i^+ \frac{\text{W-sec}}{\text{kg-cycle}} \quad (12)$$

Similarly the total energy for the negative cycle is

$$E_T^- = \sum_{i=1}^M \Delta E_i^- = \frac{1}{2mf^-} \sum_{i=1}^m SCL_i^- \frac{\text{W-sec}}{\text{kg-cycle}} \quad (13)$$

and the average power would be:

$$SCL_T = \text{specific power loss} = \frac{E_T^+ + E_T^-}{T^+ + T^-} \text{ W/kg} \quad (14)$$

Applying this technique to the 10 percent PWM square wave case we have:

Positive cycle

ORIGINAL PAGE IS  
OF POOR QUALITY

| Interval<br>( $\Delta t_i = 20 \mu s$ ) | $e_c, V$ | $\frac{d\phi}{dt}$ | We/sec | $SCL_i^+, W/kg$ |
|---|----------|--------------------|--------|-----------------|
| 1                                       | 3.4      |                    | 0.34   | 0.139           |
| 2                                       | 4.0      |                    | .40    | .202            |
| 3                                       | 3.9      |                    | .39    | .191            |
| 4                                       | 3.9      |                    | .39    | .191            |
| 5                                       | 4.0      |                    | .40    | .202            |
|   |          |                    |        | $\Sigma 0.925$  |

Negative cycle

| Interval<br>( $\Delta t_i = 100 \mu s$ ) | $e_c, V$ | $\frac{d\phi}{dt}$ | We/sec | $SCL_i^-, W/kg$  |
|--|----------|--------------------|--------|------------------|
| 1  | 0.2      |                    | 0.02   | 0.00202          |
| 2  | .4       |                    | .04    | .00968           |
| 3  | .4       |                    | .04    | .00968           |
| 4  | .4       |                    | .04    | .00968           |
| 5  | .44      |                    | .044   | .01210           |
| 6  | .5       |                    | .05    | .01628           |
| 7  | .5       |                    | .05    | .01628           |
| 8  | .55      |                    | .055   | .02002           |
| 9  | .55      |                    | .055   | .02002           |
|  |          |                    |        | $\Sigma 0.11576$ |

$$m = 5, f^+ = 5000$$

$$E_T^+ = \frac{1}{2 \times 5 \times 5000} (0.925) = 1.85 \times 10^{-5} \frac{\text{W-sec}}{\text{kg-cycle}}$$

$$m = 9, f^- = 555$$

$$E_T^- = \frac{1}{2 \times 9 \times 555} (0.11576) = 1.16 \times 10^{-5} \frac{\text{W-sec}}{\text{kg-cycle}}$$

$$SCL_T = \frac{1.85 \times 10^{-5} + 1.16 \times 10^{-5}}{100 \times 10^{-6} + 900 \times 10^{-6}} = 0.030 \text{ W/kg}$$

For the remaining cases we have:

$$\Delta t_i^+ = 20 \mu\text{s}, \quad \Delta t_i^- = 100 \mu\text{s}$$

| Duty cycle,<br>percent | $\frac{+}{T} E$ ,<br>$\frac{\text{w-sec}}{\text{kg-cycle}}$ | $\frac{+}{T}$ ,<br>$\mu\text{sec}$ | $\frac{-}{T} E$ ,<br>$\frac{\text{W-sec}}{\text{kg-cycle}}$ | $\frac{-}{T}$ ,<br>$\mu\text{sec}$ | SCL<br>$T$<br>W/kg |
|------------------------|---|------------------------------------|---|------------------------------------|--------------------|
| 20                     | $78 \times 10^{-6}$   | 200                                | $66 \times 10^{-6}$   | 800                                | 0.144              |
| 30                     | $200 \times 10^{-6}$  | 300                                | $137 \times 10^{-6}$  | 700                                | .337               |
| 40                     | $340 \times 10^{-6}$  | 400                                | $246 \times 10^{-6}$  | 600                                | .583               |
| 50                     | $397 \times 10^{-6}$  | 500                                | $365 \times 10^{-6}$  | 500                                | .762               |

A comparison of these values with the measured results is shown in Fig. 10. The error using this technique is less than that of methods 1 and 2.

The instantaneous  $p(t)$  waveforms are shown in Fig. 11. A Phillips PM3252 multiplying oscilloscope was used to obtain  $p(t)$ . In the top photo a resistive load was used to verify the accuracy of the multiplier. For the square wave the growth of  $p(t)$  is fairly linear with time, which supports the preliminary assumptions used in developing this method.

### III. General Core Loss Analysis

Analysis techniques, such as harmonic analysis and digital simulation of eddy current losses, have previously been used for prediction of core losses of distorted flux waveforms<sup>12</sup>. Eddy current correction factors<sup>13</sup> have also been employed in estimating the core loss of sinusoidal excitation considering only the fundamental and one harmonic component. In this section, method 3 of the previous section is used to analytically predict the SCL for several distorted waveform excitations.

Since this method is based upon the summation of a large number of sample points, the digital computer was used for high-speed core-loss

analysis. In order to minimize the number of subroutines of the computer algorithm, a general characteristic equation was derived using experimental data. This equation relates SCL to the equivalent frequency and  $d\phi/dt$ . An alternate equation which relates SCL to equivalent frequency and  $B_M$  was also derived. For analysis of the SCL characteristics with a specific magnetic material having a known tape or grain thickness, only a constant and two exponent values must be supplied in the initial data format.

Using the square wave SCL characteristics and the computer algorithm, analyses were performed for sinusoidal and nonsinusoidal excitation conditions using Supermalloy, Square Permalloy 80, and ferrite materials. As a final illustration of the method, the sinusoidal core-loss characteristics of a 12.7  $\mu\text{m}$  (1/2 mil) Supermalloy material operating at 1000 Hz are measured experimentally and calculated analytically.

#### (1) Development of Specific Core Loss Equations

Due to the logarithmic nature of the SCL characteristics, the SCL equation for either the  $d\phi/dt$  parameter or the  $B_M$  parameter would have the following form:

$$\text{SCL} = af_{\text{eq}}^x \quad (15)$$

The exponent  $x$  could be either positive (let  $x = d$ ) or negative (let  $x = u$ ) depending upon the parameter being examined. The constant  $a$  is also a logarithmic function of either  $d\phi/dt$  or  $B_M$ . The equation for the constant is as follows:

$$a = g(d\phi/dt)^c \quad (\text{for the } d\phi/dt \text{ parameter}) \quad (16)$$

or

$$a = s(B_M)^z \quad (\text{for the } B_M \text{ parameter}) \quad (17)$$

Combining Eq. (15) with the appropriate constant equation, the following two equation forms may be used to determine the SCL for a specific frequency and  $B_M$  or  $d\phi/dt$  level:

For  $d\phi/dt$ :

$$SCL = g(d\phi/dt)^c f_{eq}^u \quad (18)$$

For  $B_M$ :

$$SCL = s(B_M)^z f_{eq}^d \quad (19)$$

Values for the constants  $g$  and  $s$ , and for exponents  $c$ ,  $d$ ,  $z$ , and  $u$  for various magnetic materials were determined from the experimental data. These calculated values are shown in Tables I and II. In Eq. (19) at low flux densities, the  $d$  exponent was determined by Steinmetz to be 1.6 for electrical sheet steel<sup>14</sup>. For higher flux densities the value of the exponent may be as high as 2.5. The values of the exponent as measured in these experiments fall within this upper limit. The value of the exponent was found to be dependent upon both the magnetic material and the tape thickness.

The use of Eq. (18) and (19) is not restricted to computer algorithm. By using a simple hand calculator and the analysis method described in section II (3), the SCL for a particular magnetic material and tape thickness may easily be determined. An example of this process is shown in Fig. 12. For the waveform shown the positive half cycle frequency is 8.77 kHz, and the negative half cycle frequency is 12.5 kHz. The measured SCL for this waveshape is 0.317 W/kg. If the SCL is calculated using 5  $\mu$ s intervals, the calculated value is 0.290 W/kg. This represents an error of 8.3 percent. This error will be reduced by decreasing the sample interval.

The same example shown in Fig. 12 was recalculated using the computer algorithm with the sample interval decreased to 2  $\mu$ s. The calculated SCL for this example was calculated as 0.312 W/kg. This represents an error of only 1.6 percent when compared with the experimentally measured SCL of 0.317 W/kg.

This example demonstrates that the third method developed in section II may be used to determine the SCL for highly distorted waveforms. Also, by decreasing the sample interval the accuracy of the analysis will be improved.

## (2) Examples

In this section five examples are presented which demonstrate the accuracy of the incremental  $d\phi/dt$  method. Three magnetic materials were used in the analysis with experimental measurement of their SCL made under both sinusoidal and nonsinusoidal excitation. The waveforms used in these analyses are shown in Fig. 13. Both ferrite 3B7 material and Square Permalloy 80 were analyzed using these waveforms. The results of these SCL analyses are shown below:

| Material            | Sinusoidal excitation |            | Nonsinusoidal excitation |            |
|---------------------|-----------------------|------------|--------------------------|------------|
|                     | Calculated            | Measured   | Calculated               | Measured   |
| Ferrite             | 0.854 W/kg            | 0.812 W/kg | 0.537 W/kg               | 0.543 W/kg |
| Square Permalloy 80 | 1.709 W/kg            | 1.575 W/kg | 1.956 W/kg               | 1.828 W/kg |

The percentages of error shown for these examples are consistent with those measured for the previous examples. Therefore this method may be used for analysis over the wide range of excitation conditions encountered in the application of the magnetic materials.

This method may also be used with the square wave SCL characteristics to determine the SCL characteristics for sinusoidal excitation. Figure 14 shows the results of an analysis of a 1000 Hz sine wave for various  $B_M$  levels. The calculated results shown as a bold line are compared with the measured sinusoidal characteristics for 12.7  $\mu m$  (1/2 mil) Supermalloy material. The results show that an extremely accurate SCL characteristic may be achieved by this method of analysis.

#### IV. Conclusion

Application of power electronics technology is having a significant impact on the design of, and energy use in, present and future power systems. Since the management of electrical energy has become an area of increasing concern, the optimal design of key power train components is extremely important. One of the major components within such a power system is the magnetic device. This component is used for voltage and current transformation, input/output filter sections, parameter sensing, and semiconductor control.

The research covered in this paper provides the power electronics designer with a unique analytical tool for investigation of the core-loss characteristics of magnetic materials. Analysis methods previously available were based strictly on sinusoidal excitation voltages. Core-loss analysis has been based on the assumption that eddy current and hysteresis loss components are separable. By using a novel excitation technique employing a pulse-width modulated square wave, a true separation of these two loss components was shown experimentally. This approach provides a straightforward analysis technique to characterize the basic core-loss process of new materials.

For fixed  $B_M$  conditions the width of the B-H locus may be constructed for any type of waveform excitation. This approach was used to explain the observed difference in B-H width when excited from either a voltage source (narrow B-H width) or a current source (wider B-H width). The flux characteristics under these two source conditions directly influence the observed B-H shape. For sinusoidal voltage excitation the flux is cosinusoidal in shape and has variable  $d\phi/dt$  values over one cycle. For sinusoidal current excitation the flux approaches a square wave. This excitation causes correspondingly higher  $d\phi/dt$  values than those encountered for cosinusoidal flux conditions.

These results demonstrate the advantage of using square wave excitation as an analysis tool to determine core-loss characteristics. In addition, with square wave excitation the application of Faraday's Law becomes straightforward as  $d\phi/dt$  is a constant value. The SCL characteristics were experimentally measured by holding  $d\phi/dt$  constant and varying frequencies to develop a family of core-loss characteristics.

Core excitations involving symmetric conditions for both sinusoidal and square waveforms were investigated analytically using the new incremental time rate of change of flux method. Experimental data was used to check the accuracy of this method. The predicted and measured specific losses were within eight percent of each other for all conditions analyzed. This deviation is within the error band of the instrumentation. Therefore, this method provides a set of magnetic characteristics for a specific magnetic material, core configuration, and tape thickness which is easily understood and accurately predicts the SCL for any type of voltage excitation encountered in dc-ac/dc converter configurations.

### References

- [1] G. N. Glasco, and J. V. Lebacqz, Pulse Generators. McGraw-Hill Book Co., Inc., New York, 1948.
- [2] J. Smit, Magnetic Properties of Materials. McGraw-Hill Book Co., Inc., New York, 1971.
- [3] Design Manual Featuring Tape Wound Cores. Magnetics, Inc., TWC-300R.
- [4] D. Y. Chen, "Comparisons of High Frequency Magnetic Core Losses Under Two Different Driving Conditions. A Sinusoidal Voltage and a Square Wave Voltage," pp. 237-241 in I.E.E.E. Power Electronics Specialist Conference, Syracuse, N.Y., 1978.
- [5] W. H. Hayt, Engineering Electromagnetics. McGraw-Hill Book Co., Inc., New York, 1967.
- [6] T. H. Putnam, "Economics of Power Transformer Design," IEEE Trans. Power Appar. Syst., 82 [12] 1018-1023 (1963).
- [7] F. C. Lee, Y. Yu, and J. E. Triner, "Power Converter Design Optimization," pp. 104-112 in IEEE Power Electronics Specialists Conference, Palo Alto, Ca., 1977.
- [8] E. F. W. Alexanderson, "Magnetic Properties of Iron at Frequencies up to 200,000 Cycles," AIEE Transactions, 30 [3] 2433-2454 (1911).
- [9] C. R. Boon, and J. A. Robey, "Effect of Domain Wall Motion on Power Loss in Grain Oriented Silicon-Iron Sheet," IEEE Proc. 115 [10] 1535-1540 (1968).
- [10] J. D. Lavers, P. P. Biringer, and H. Hollitscher, "A Simple Method of Estimating the Minor Loop Hysteresis Loss in Thin Laminations," IEEE Trans. Magn., MAG-14 [5] 386-388 (1978).
- [11] K. J. Overshott, "The Use of Domain Observations in Understanding and Improving the Magnetic Properties of Transformer Steels," IEEE Trans. Magn., MAG-12 [6] 840-845 (1976).

- [12] J. D. Lavers, and P. P. Biringer, "Prediction of Core Losses for High Flux Densities and Distorted Flux Waveforms," IEEE Trans. Magn., MAG-12 [6] 1053-1055 (1976).
- [13] J. D. Lavers, P. P. Biringer, and H. Hollitscher, "Estimation of Core Losses When the Flux Waveform Contains the Fundamental Plus a Single Odd Harmonic Component," IEEE Trans. Magn., MAG-13 [5] 1128-1130 (1977).
- [14] R. P. Ward, Introduction to Electrical Engineering. Prentice Hall, Inc., New York, 1952.

TABLE I. - TABULATION OF THE CONSTANT AND EXPONENT  
VALUES USED IN EQUATION (18)

| Constant | Tape thickness, $\mu\text{m}$ , (mils) |                     |                     |
|----------|--|---------------------|---------------------|
|          | 12.7 (0.5)                             | 25.4 (1.0)          | 50.8 (2.0)          |
| c        | 2.270                                  | 1.563               | 1.981               |
| g        | $7.536 \times 10^3$                    | $2.681 \times 10^3$ | $5.023 \times 10^1$ |
| u        | -1.000                                 | -0.811              | -0.500              |
|          |  |                     | -0.345              |

(a) Supermalloy-Cut Core

| Constant | Tape thickness, $\mu\text{m}$ , (mils) |                     |                     |
|----------|--|---------------------|---------------------|
|          | 12.7 (0.5)                             | 25.4 (1.0)          | 50.8 (2.0)          |
| c        | 1.951                                  | 2.000               | 2.090               |
| g        | $6.673 \times 10^3$                    | $9.740 \times 10^3$ | $3.763 \times 10^2$ |
| u        | -0.408                                 | -0.825              | -0.561              |
|          |  |                     | -0.297              |

(b) Supermalloy-Uncut

| Constant | Tape thickness, $\mu\text{m}$ , (mils) |                     |                     |
|----------|--|---------------------|---------------------|
|          | 12.7 (0.5)                             | 25.4 (1.0)          | 50.8 (2.0)          |
| c        | 0.985                                  | 1.713               | 1.704               |
| g        | $3.070 \times 10^2$                    | $3.070 \times 10^2$ | $1.132 \times 10^2$ |
| u        | -0.349                                 | -0.225              | -0.226              |
|          |  |                     | -0.258              |

(c) Square Permalloy 80-Uncut

| Constant | Tape thickness, $\mu\text{m}$ , (mils) |                     |                     |
|----------|--|---------------------|---------------------|
|          | 12.7 (0.5)                             | 25.4 (1.0)          | 50.8 (2.0)          |
| c        | 0.985                                  | 1.739               | 1.739               |
| g        | $3.079 \times 10^2$                    | $3.070 \times 10^2$ | $1.132 \times 10^2$ |
| u        | -0.349                                 | -0.225              | -0.226              |
|          |  |                     | -0.258              |

TABLE II. - TABULATION OF THE CONSTANT AND EXPONENT  
VALUES USED IN EQUATION (18)

(a) Supermalloy-Cut Core

| Constant | Tape thickness, $\mu\text{m}$ , (mils) |                        |                        |
|----------|--|------------------------|------------------------|
|          | 12.7 (0.5)                             | 25.4 (1.0)             | 50.8 (2.0)             |
| z        | 2.038                                  | 2.084                  | 1.948                  |
| s        | $8.979 \times 10^{-4}$                 | $5.079 \times 10^{-4}$ | $1.089 \times 10^{-4}$ |
| d        | 1.210                                  | 1.307                  | 1.670                  |

(b) Supermalloy-Uncut

| Constant | Tape thickness, $\mu\text{m}$ , (mils) |                        |                        |
|----------|--|------------------------|------------------------|
|          | 12.7 (0.5)                             | 25.4 (1.0)             | 50.8 (2.0)             |
| z        | 1.940                                  | 2.000                  | 2.110                  |
| s        | $5.440 \times 10^{-4}$                 | $1.909 \times 10^{-4}$ | $5.804 \times 10^{-5}$ |
| d        | 1.230                                  | 1.300                  | 1.530                  |
|          |  |                        | 1.750                  |

(c) Square Permalloy 80-Uncut

| Constant | Tape thickness, $\mu\text{m}$ , (mils) |                        |                        |
|----------|--|------------------------|------------------------|
|          | 12.7 (0.5)                             | 25.4 (1.0)             | 50.8 (2.0)             |
| z        | 0.976                                  | 1.696                  | 1.722                  |
| s        | $3.050 \times 10^{-2}$                 | $9.438 \times 10^{-5}$ | $1.246 \times 10^{-4}$ |
| d        | 0.624                                  | 1.456                  | 1.459                  |
|          |  |                        | 1.1613                 |

| Constant | Material            | Material            |
|----------|---------------------|---------------------|
| c        | 3B7                 | 3B7                 |
| g        | $4.478 \times 10^6$ | $4.478 \times 10^6$ |
| u        | -1.6                | -1.6                |

ORIGINAL PAGE IS  
OF POOR QUALITY

**ORIGINAL PAGE IS  
OF POOR QUALITY**

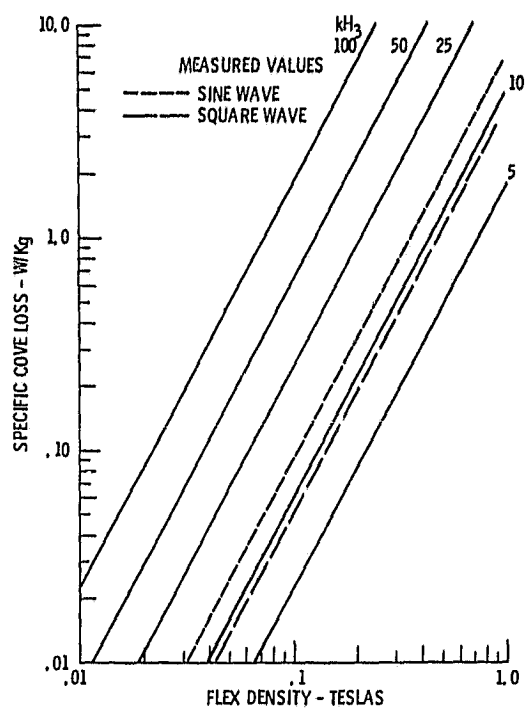
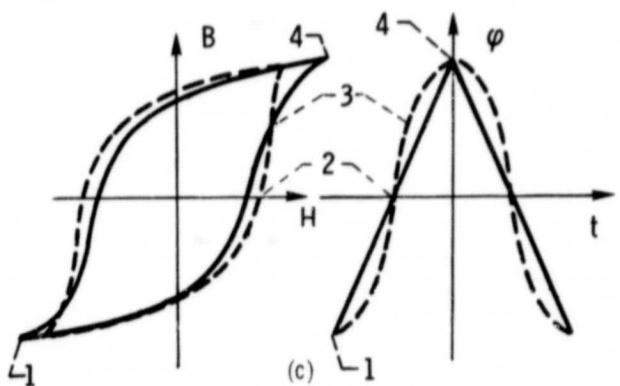
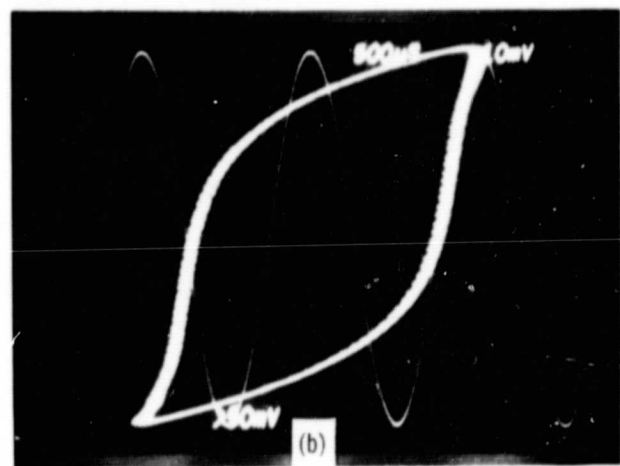
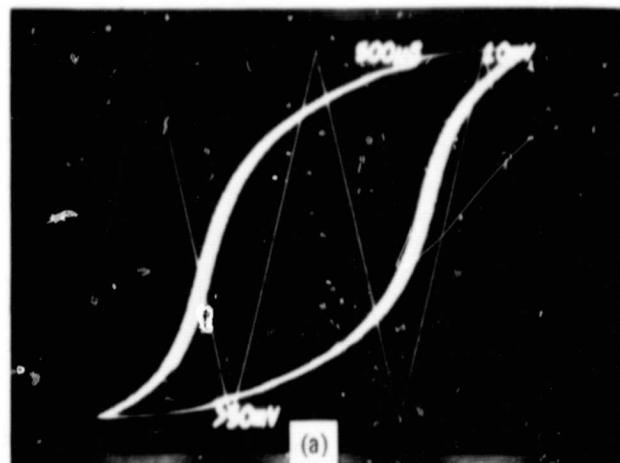


Figure 1. - Specific core loss characteristics from magnetics Inc data

ORIGINAL PAGE  
BLACK AND WHITE PHOTOGRAPH



(a) B-H loop with  $d\phi/dt = k$ .

(b) B-H loop with  $d\phi/dt = k(t)$ .

(c) Superimposed B-H loops and flux excitations for constant and variable  $d\phi/dt$  conditions.

Figure 2. - Comparison of B-H loop characteristics for constant and variable  $d\phi/dt$  conditions with frequency and  $B_m$  as a constant.

ORIGINAL PAGE IS  
OF POOR QUALITY

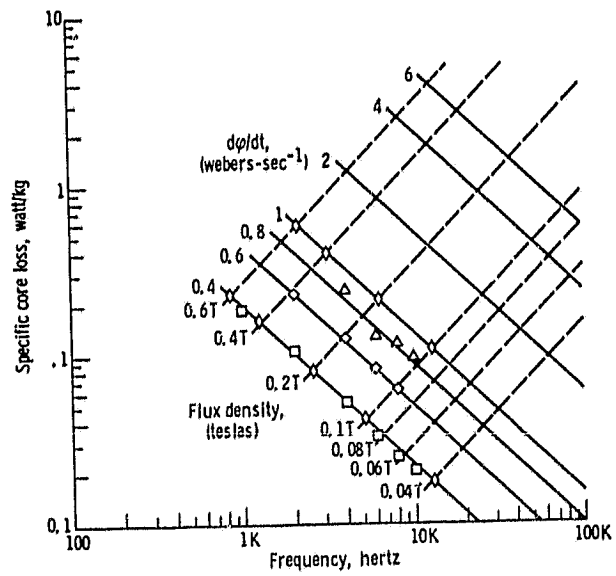


Figure 3. - Specific core loss characteristics for cut 12.7  $\mu$ m (1/2 mil)  
Supermalloy for square wave excitation with  $B_M$  and  $d\phi/dt$  as para-  
meters.

ORIGINAL PAGE IS  
OF POOR QUALITY

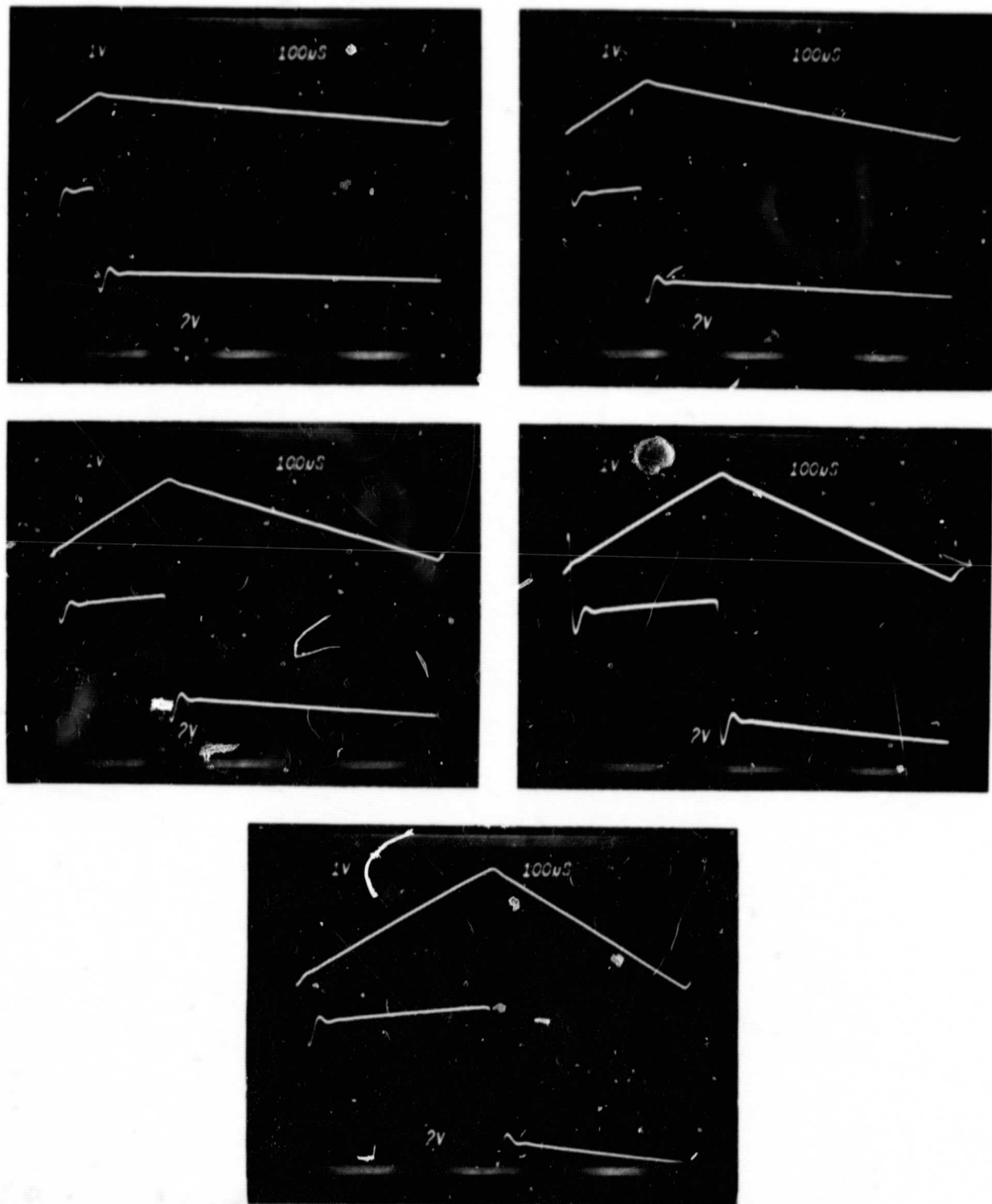


Figure 4. - Waveform excitation for a pulse width modulated square wave.

ORIGINAL PAGE IS  
OF POOR QUALITY

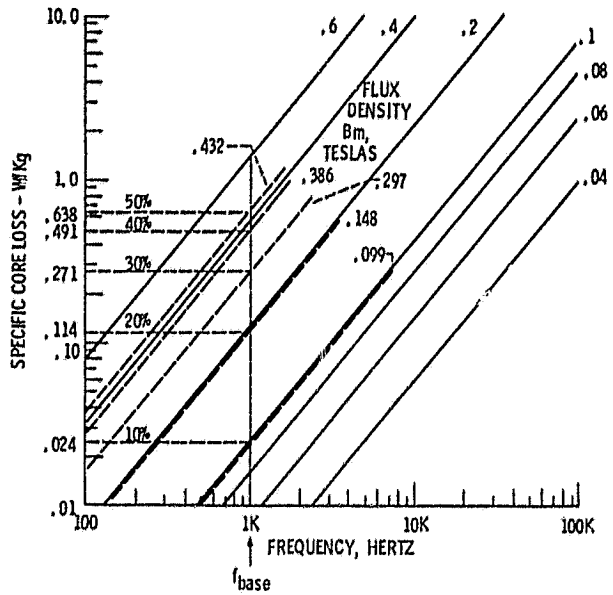


Figure 5. - Specific core loss characteristics for cut  $12.7 \mu\text{m}$  (1/2 mil)  
Superalloy under duty cycle conditions.

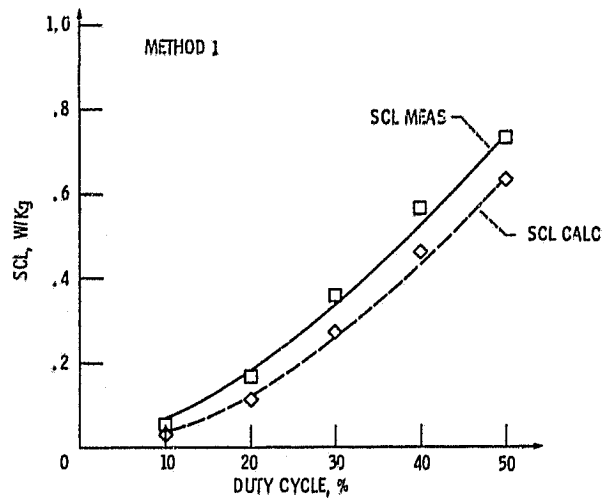
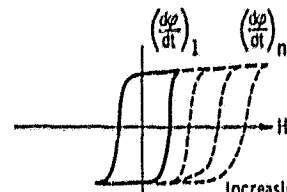
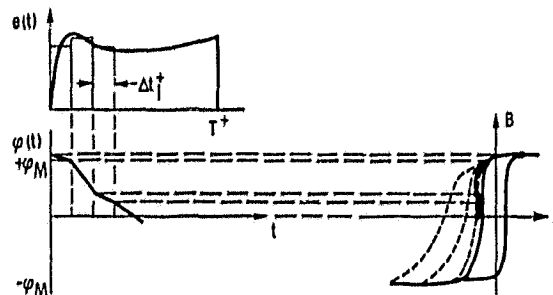


Figure 6. - Comparison of calculated vs measured values of SCL for  
for  $12.7 \mu\text{m}$  (1/2 mil) superalloy as a function of duty cycle for a  
1 kHz-3.9 volt pulse voltage.

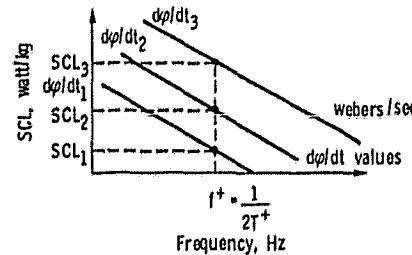
ORIGINAL PAGE IS  
OF POOR QUALITY



(a) Family of curves for various  $d\phi/dt$  values.



(b) Relationship of incremental  $d\phi/dt$  rates to B-H loop.



(c) SCL characteristics for various  $d\phi/dt$  values.

Figure 9. - Family of B-H loops and SCL characteristics based on  $d\phi/dt$  as a parameter.

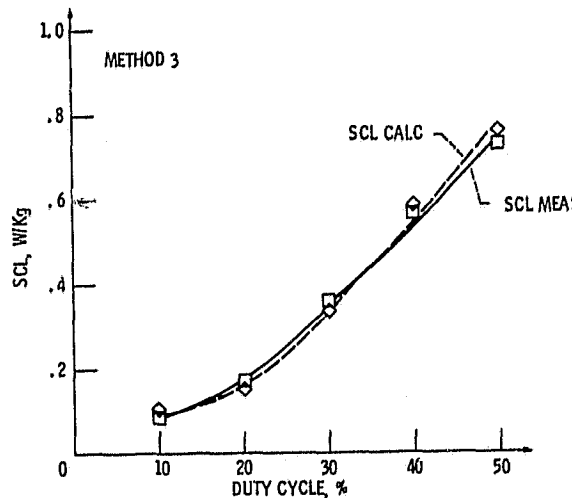


Figure 10. - Comparison of calculated vs measured values of SCL as a function of duty cycle for 1 kHz - 3.9 volt pulse voltage.

ORIGINAL PAGE IS  
OF POOR QUALITY

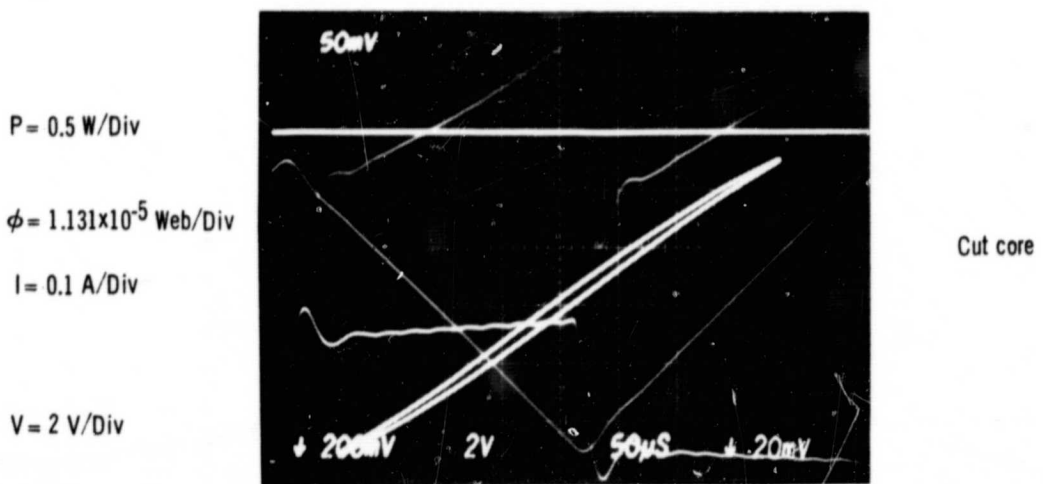
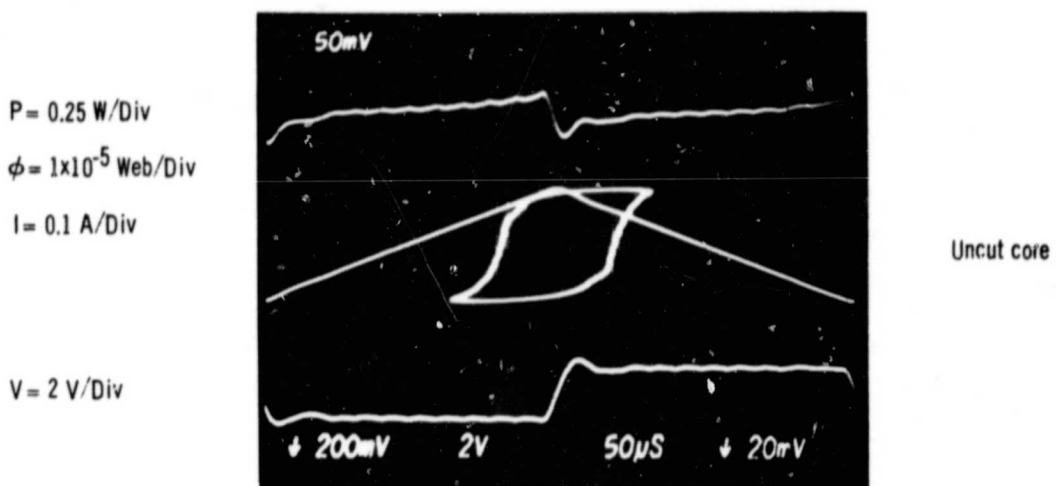
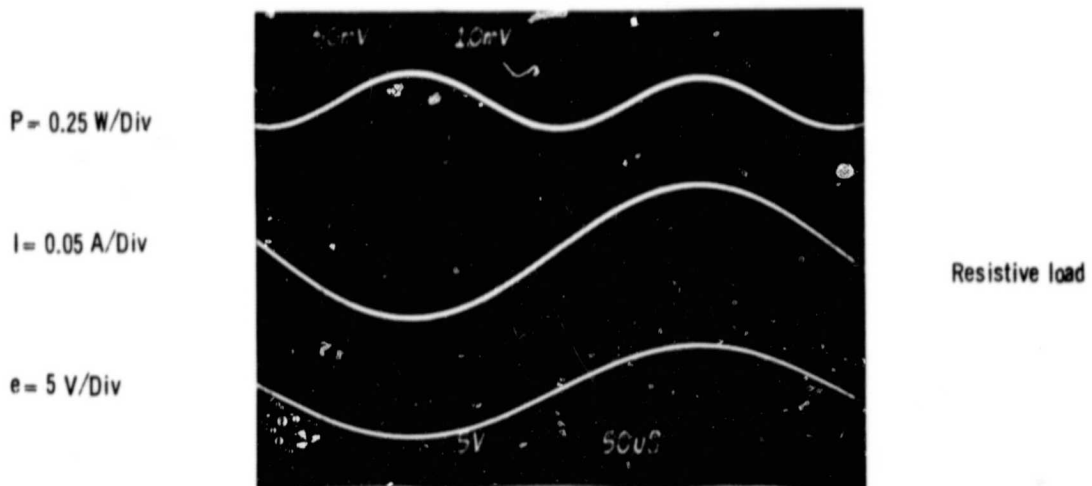
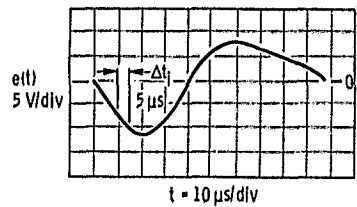


Figure 11. - Instantaneous energy characteristics.

ORIGINAL PAGE IS  
OF POOR QUALITY.



Waveform excitation into a 12.7  $\mu\text{m}$   
(1/2 mil) Supermalloy cut core

$$\text{SCL} = 7.536 \times 10^3 (\frac{d\phi}{dt})^2 \cdot 27 f_{\text{eq}}^{-1} \quad (4.3)$$

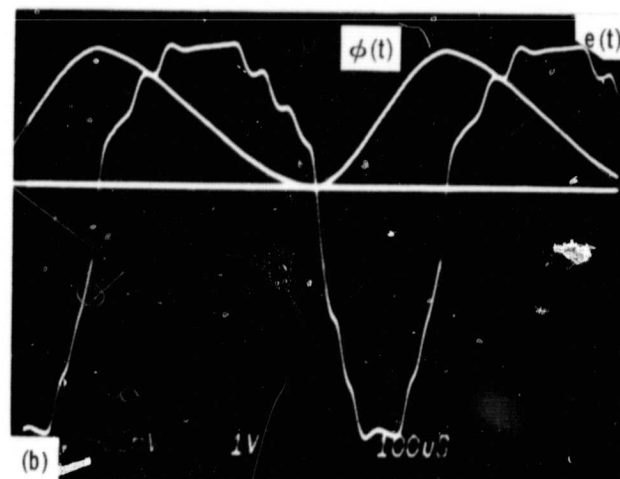
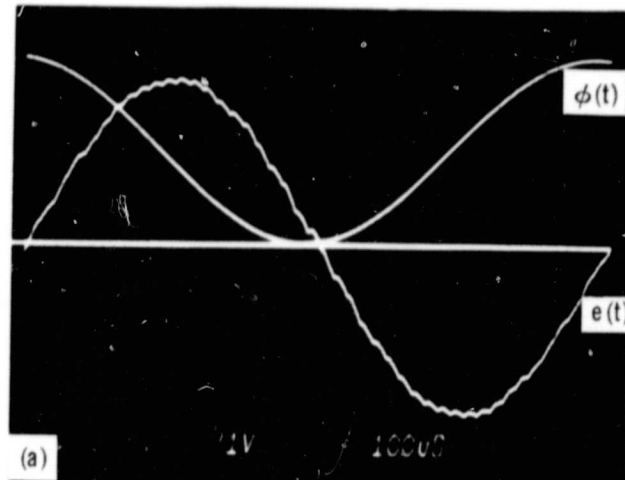
|                       | Internal | $e(t) - V$ | $\frac{d\phi}{dt} - \text{webers/sec}$ | SCL, watt/kg |
|-----------------------|----------|------------|--|--------------|
| -ive<br>half<br>cycle | 1        | 0          | 0                                      | 0            |
|                       | 2        | 2.5        | 0.25                                   | 0.029        |
|                       | 3        | 6.5        | 0.65                                   | 0.242        |
|                       | 4        | 9.5        | 0.95                                   | 0.574        |
|                       | 5        | 11.5       | 1.15                                   | 0.887        |
|                       | 6        | 11.0       | 1.10                                   | 0.801        |
|                       | 7        | 8.5        | 0.85                                   | 0.447        |
|                       | 8        | 5          | 0.05                                   | 0            |
| +ive<br>half<br>cycle | 1        | 0          | 0                                      | 0            |
|                       | 2        | 3          | 0.30                                   | 0.059        |
|                       | 3        | 6.5        | 0.65                                   | 0.345        |
|                       | 4        | 8.2        | 0.82                                   | 0.585        |
|                       | 5        | 8.0        | 0.80                                   | 0.653        |
|                       | 6        | 7.0        | 0.70                                   | 0.409        |
|                       | 7        | 6.5        | 0.65                                   | 0.345        |
|                       | 8        | 5.8        | 0.58                                   | 0.266        |
|                       | 9        | 5.0        | 0.50                                   | 0.191        |
|                       | 10       | 3.5        | 0.35                                   | 0.086        |
|                       | 11       | 3.0        | 0.30                                   | 0.059        |
|                       | 12       | 1.0        | 0.10                                   | 0.004        |
|                       | 13       | 0          | 0                                      | 0            |

Using equation 3.16:

$$\text{SCL}_T = \frac{\frac{2.98}{2x8 \times 12.5 \times 10^3} + \frac{3.00}{2x13 \times 8.77 \times 10^3}}{96.9 \times 10^{-6}} = 0.289 \text{ watt/kg}$$

Figure 12. - An example to demonstrate the application of method 3 and the specific core loss equations.

ORIGINAL PAGE IS  
OF POOR QUALITY



(a) Sinusoidal excitation.

(b) Nonsinusoidal excitation.

Figure 13. - Waveform excitation for sinusoidal and nonsinusoidal conditions.

ORIGINAL PAGE IS  
OF POOR QUALITY

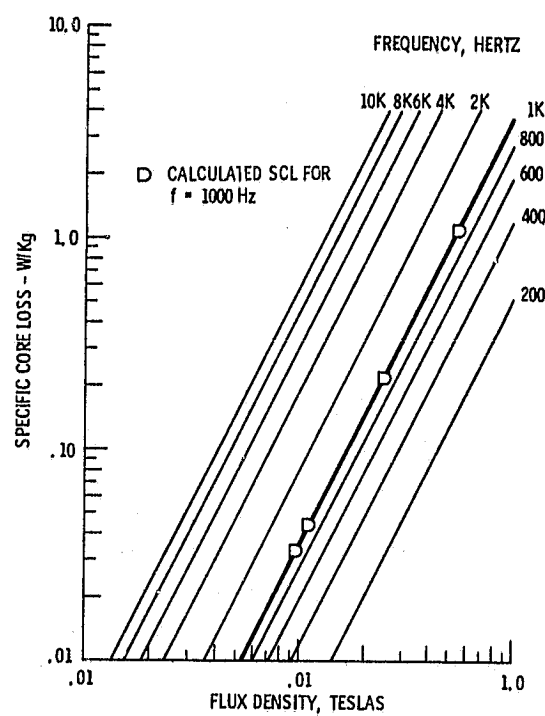


Figure 14. - Comparison of calculated and measured results for specific core loss of 1/2 mill cut supermalloy under sinusoidal excitation at 1000 Hz.